Electronic Supplementary Material (ESI) for Journal of Materials Chemistry A.

Supplementary Information

Hydrogen and Methane Storage and Release by MoS_2 Nanotubes for Energy Storage

Xiuxiu Wang[1], Baoyu Li[1], David R. Bell[2], Weifeng Li[1,*], and Ruhong Zhou[2,3,*]

1. School for Radiological and Interdisciplinary Sciences (RAD-X) and Collaborative Innovation Center of Radiation Medicine of Jiangsu Higher Education Institutions, Soochow University, Suzhou, China, 215123

2. Computational Biological Center, IBM Thomas J. Watson Research Center, Yorktown Heights, NY 10598, USA

3. Department of Chemistry, Columbia University, New York, NY 10027, USA

E-mails: wfli@suda.edu.cn (W. F. Li) and ruhongz@us.ibm.com (R. H. Zhou)

1. Methane Adsorption Energy Profiles by MD and Quantum Mechanics Calculations

To check the validity of the classical MoS_2 model, we have considered a representative case – the adsorption of CH_4 onto a MoS_2 monolayer along the perpendicular direction. Specifically, the CH_4 molecule was initially placed ~0.8 nm away from the MoS_2 monolayer (measured from the C of CH_4 to the outmost S of MoS_2) and moved towards the S atom, during which the total potential energy of the system was monitored by both classical MD calculations (with GROMACS) and quantum chemistry (QM) calculations (with the Vienna ab initio simulation package, VASP[1, 2]). In the QM calculations, the projector-augmented wave (PAW) potentials[3] were used to take into account the electron-ion interactions, while the electron exchange-correlation interactions were treated using the generalized gradient approximation (GGA)[4] in the form of Perdew-Burke-Ernzerhof (PBE) scheme. In order to correctly describe van der Waals interactions between MoS_2 and CH_4, a correction term (DFT-D2 method of Grimme[5]) is added when calculating the conventional Kohn-Sham potential energy and interatomic forces. This correction has been well documented to be the best exchange-correlation functional to represent the structure energetics of graphite systems[6]. A plane-wave cutoff of 500 eV was used for all the calculations. A supercell composed of 4 × 4 lateral periodicity of MoS_2 was adopted with a vacuum of 3 nm being placed in the z-direction to avoid mirror interactions. The z-component of separation between the S and C atoms was restrained to certain values from 0.8 nm to 0 nm in increments of 0.02 nm. The geometry and orientation of CH_4 were fully optimized using a conjugate gradient algorithm to obtain the ground-state configuration. Atomic relaxation was performed until the change of total energy was smaller than 0.01 meV and all the Hellmann-Feynman forces on each atom were less than 0.1 eV/Å, which guarantees fully relaxed structures. A k-point sampling of 7 × 7 × 1 was used in all calculations.

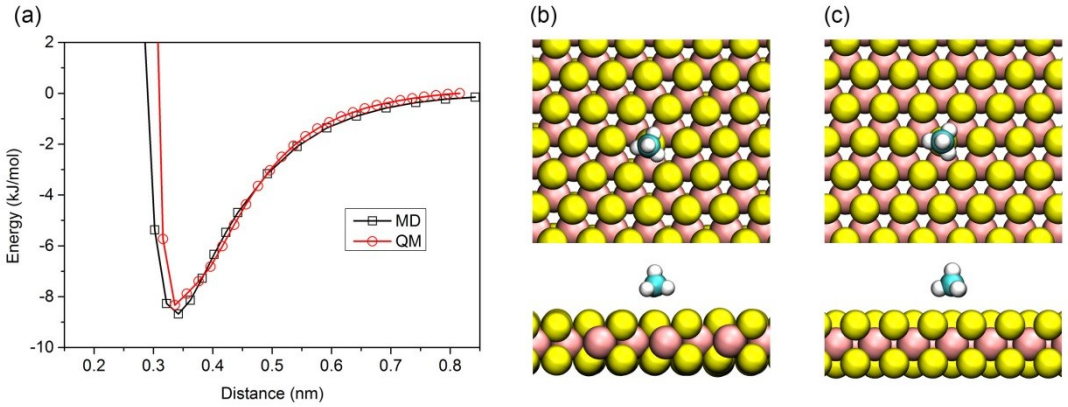

Figure S1. (a) Adsorption energy profiles between MoS_2 monolayer and a methane molecule as a function of vertical separation from MD and QM calculations (T = 0 K); (b) The top view and side view of methane orientation on MoS_2 from MD and (c) The top view and side view of methane orientation on MoS_2 from QM calculation.

The two adsorption energy profiles of CH_4 on MoS_2 are summarized in Fig. S1a. The results indicate that our classic MoS_2 model can reasonably reproduce the interaction obtained from QM calculations, both in the shape of curves and the depth of energy wells. Furthermore, the MD and QM calculations result in consistent structures (Fig. S1b and S1c): the CH_4 has one C-H bond pointing along the normal direction of MoS_2 monolayer. The other three C-H bonds point towards neighboring S atoms.

2. Time Constant for Gas Adsorption

The representative gas adsorption processes in Fig. S2-S5 are quantitatively analyzed by calculating the time constant for gas adsorption. In detail, the profiles of number of adsorbed gas molecules are mathematically fitted with an exponential formula

$$y = A - \alpha \times e^{-\frac{t}{\tau}}$$

where A stands for the average number of adsorbed gas molecules, τ stands for the time constant for adsorption process. Here, a larger value of time constant means a longer adsorption rate.

Table S1 summarizes the fitted parameters for the representative gas adsorption in Fig. S2-S5. First, the time constant τ generally decreases with respect to pressure increase. We attribute this to the effect of gas density on the gas adsorption process, where low density gas (low pressure) requires a longer time to bind to MoS_2 NT to reach an equilibrium state. Second, the time constants for hydrogen adsorption are generally smaller than that for methane. This is mainly because hydrogen gas molecules have larger velocities than methane at same temperature.

The only case that is worth noticing is H_2@(6, 6) at 1 MPa, which has a significantly large time constant of 492.6 ps. This phenomenon is caused by the formation of linear hydrogen chain inside (6, 6) NT as demonstrated in Fig. 3c in the main manuscript. At the extreme condition of 1 MPa considered in our present study, such a hydrogen chain can still be spontaneously formed. Because of the space confinement of the MoS_2 NT, hydrogen gas can only intrude into the NT interior in sequential order, resulting in a considerably large time constant. For H_2@(6, 6) at 5 and 10 MPa, such a hydrogen chain is also observed. However, due to the large number of rapid hydrogen adsorption to the MoS_2 NT surface, the slow hydrogen chain formation only plays a negligible role when calculating time constants for 5 and 10 MPa.

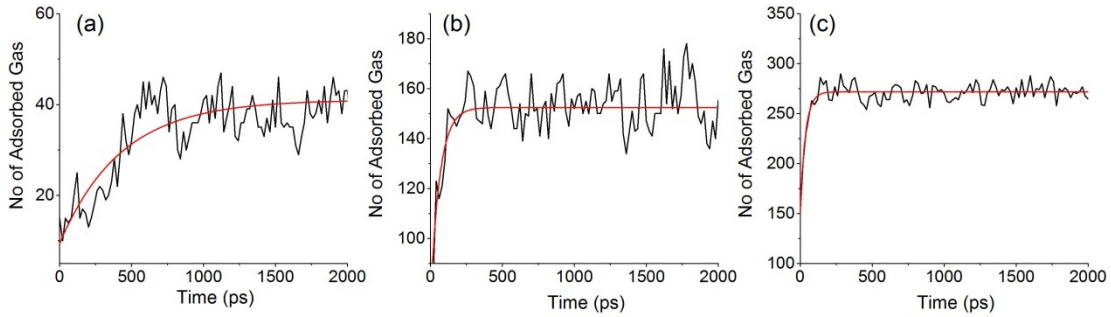

Figure S2. Time evolutions of total number of methane molecules bound to (12, 12) MoS_2 NT at (a) 1 MPa, (b) 5 MPa and (c) 10 MPa at 175 K.

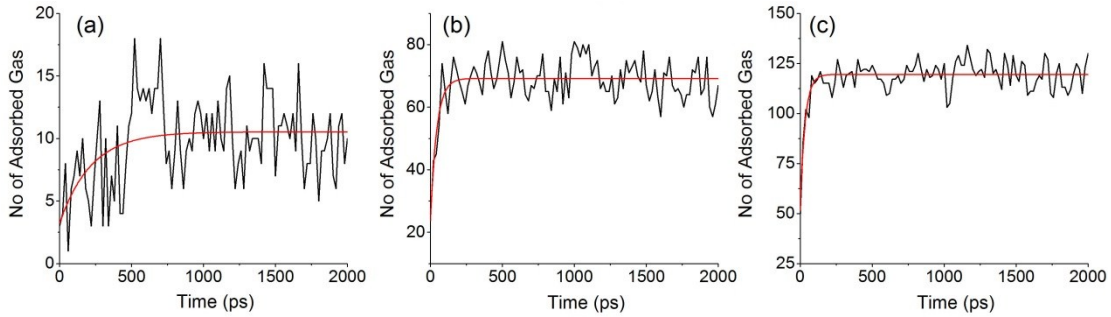

Figure S3. Time evolutions of total number of methane molecules bound to (6, 6) MoS_2 NT at (a) 1 MPa, (b) 5 MPa and (c) 10 MPa at 175 K.

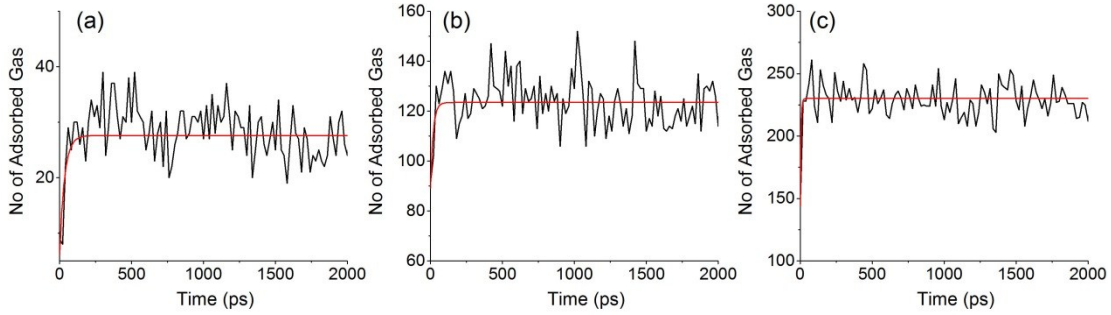

Figure S4. Time evolutions of total number of hydrogen molecules bound to (12, 12) MoS_2 NT at (a) 1 MPa, (b) 5 MPa and (c) 10 MPa at 175 K.

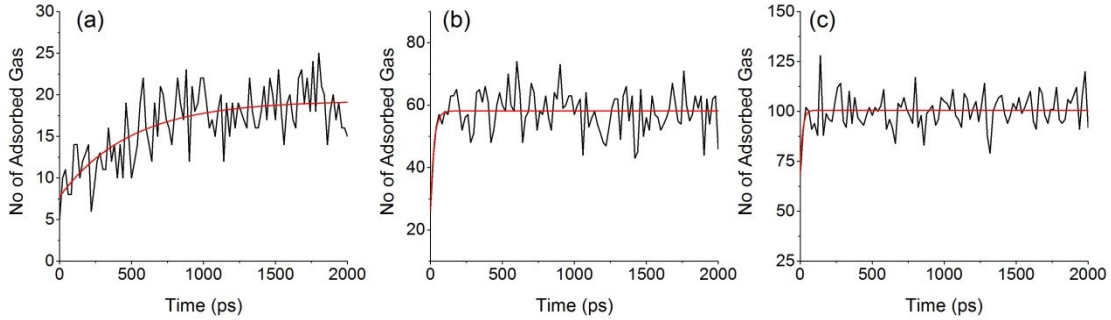

Figure S5. Time evolutions of total number of hydrogen molecules bound to (6, 6) MoS_2 NT at (a) 1 MPa, (b) 5 MPa and (c) 10 MPa at 175 K.

Table S1. Fitted parameters of A and τ for the gas adsorption process in Fig. S2-S5.

	Pressure (MPa)	A	τ (ps)
CH_4@(12, 12)	1	40.0	423.7
	5	152.4	62.8
	10	271.8	35.7
CH_4@(6, 6)	1	10.5	218.3
	5	69.2	42.9
	10	119.4	33.3
H_2@(12, 12)	1	27.6	33.5
	5	123.4	18.6
	10	230.2	5.5
H_2@(6, 6)	1	19.3	492.6
	5	58.1	23.1
	10	100.5	15.9

3. Binding Energy Profiles of Gas Dimer

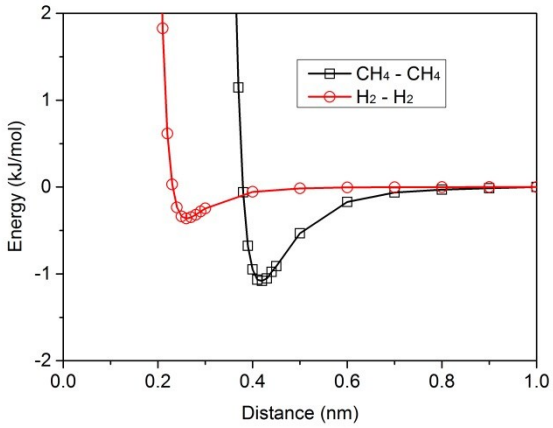

Figure S6. Binding energy profiles between two CH_4 and H_2, respectively, from MD calculations (T = 0 K).

The interactions of two CH_4 and H_2 were explored by MD calculations to explain the formation of two binding shells of CH_4 around MoS2 NTs. At T = 0 K, the energy minimum separation between two CH_4 is 0.42 nm with binding energy of -1.08 kJ/mol. For the H_2 dimer, the separation is 0.25 nm with weaker binding energy of -0.33 kJ/mol.

References:

1. G. Kresse and J. Furthmuller, *Phys. Rev. B*, 1996, **54**, 11169-11186.
2. G. Kresse and J. Furthmuller, *Comput. Mater. Sci.*, 1996, **6**, 15-50.
3. P. E. Blochl, *Phys. Rev. B*, 1994, **50**, 17953-17979.
4. J. P. Perdew, J. A. Chevary, S. H. Vosko, K. A. Jackson, M. R. Pederson, D. J. Singh and C. Fiolhais, *Phys. Rev. B*, 1992, **46**, 6671-6687.
5. L. Britnell, R. V. Gorbachev, R. Jalil, B. D. Belle, F. Schedin, A. Mishchenko, T. Georgiou, M. I. Katsnelson, L. Eaves, S. V. Morozov, N. M. R. Peres, J. Leist, A. K. Geim, K. S. Novoselov and L. A. Ponomarenko, *Science*, 2012, **335**, 947-950.
6. N. Myoung, K. Seo, S. J. Lee and G. Ihm, *ACS Nano*, 2013, **7**, 7021-7027.